

# Catalytic conversion of N<sub>2</sub>O to N<sub>2</sub> over metal-based catalysts in the presence of hydrocarbons and oxygen

S.C. Christoforou \*, E.A. Efthimiadis, and I.A. Vasalos

*Centre for Research and Technology Hellas, Chemical Process Engineering Research Institute, P.O. Box 1517, 54006 University City, Thessaloniki, Greece*

Received 11 September 2001; accepted 3 January 2002

The catalytic conversion of N<sub>2</sub>O to N<sub>2</sub> in the presence or the absence of propene and oxygen was studied. The catalysts examined in this work were synthesized impregnating metals (Rh, Ru, Pd, Co, Cu, Fe, In) on different supports (Al<sub>2</sub>O<sub>3</sub>, SiO<sub>2</sub>, TiO<sub>2</sub>, ZrO<sub>2</sub> and calcined hydrotalcite MgAl<sub>2</sub>(OH)<sub>8</sub>·H<sub>2</sub>O). The experimental results varied both with the type of the active site and with the type of the support. Rh and Ru impregnated on  $\gamma$ -alumina exhibited the highest activity. The performance of the above most promising catalysts was studied using various hydrocarbons (CH<sub>4</sub>, C<sub>3</sub>H<sub>6</sub>, C<sub>3</sub>H<sub>8</sub>) as reducing agents. These experimental results showed that the type of reducing agent does not affect the reaction yield. The temperature where complete conversion of N<sub>2</sub>O to N<sub>2</sub> was measured was independent of the reductant type. The activity of the most active catalysts was also measured in the presence of SO<sub>2</sub> and H<sub>2</sub>O in the feed. A shift of the N<sub>2</sub>O conversion *versus* temperature curve to higher temperatures was observed when SO<sub>2</sub> and H<sub>2</sub>O were added, separately or simultaneously, to the feed. The inhibition caused by SO<sub>2</sub> was attributed to the formation of sulfates and that caused by water to the competitive chemisorption of H<sub>2</sub>O and N<sub>2</sub>O on the same active sites.

**KEY WORDS:** N<sub>2</sub>O; nitrous oxide; reduction; decomposition; Rh; Ru; SO<sub>2</sub>; H<sub>2</sub>O.

## 1. Introduction

N<sub>2</sub>O emitted from anthropogenic sources contributes to the greenhouse effect and to the destruction of the ozone layer. N<sub>2</sub>O is present in relatively low concentrations in the troposphere (about 310 ppb); however, it is included in the powerful greenhouse gases. N<sub>2</sub>O is very stable in air and its atmospheric lifetime is *ca.* 150 years. The atmospheric concentration of N<sub>2</sub>O increases at a rate of about 0.37% per year. The only way to decrease the N<sub>2</sub>O emissions is to limit the emissions derived from anthropogenic activities. Chemical processes associated with the production and use of nitric acid and fluidized bed combustion are two of the main nitrous oxide sources, since their contribution to the total N<sub>2</sub>O emissions is about 20% [1]. The public awareness and sensitivity on environmental issues motivated the European Union to commit itself to reduce the greenhouse gases by 5–8% by 2012. This implies that the development of an efficient technology for control of N<sub>2</sub>O emissions is a priority.

The catalytic decomposition and the selective catalytic reduction (SCR) of N<sub>2</sub>O to N<sub>2</sub> are two candidate technologies, which can be applied to reduce the emissions of this harmful gas. The selective catalytic reduction of N<sub>2</sub>O was studied only over Cu/ZSM-5 and Fe/ZSM-5 catalysts [2–5]. Both catalysts exhibited high activity

under ideal reaction conditions (absence of poison gases). Fe/ZSM-5 maintained most of its initial activity after the addition of H<sub>2</sub>O to the feed, while the H<sub>2</sub>O presence caused a shift of the N<sub>2</sub>O conversion *versus* temperature curve to higher temperatures over Cu/ZSM-5. Centi and Vazzana [3] examined the tolerance and the durability of Fe/ZSM-5 for the N<sub>2</sub>O reduction using a feed that simulated flue gases (presence of O<sub>2</sub>, H<sub>2</sub>O and SO<sub>2</sub>). About 60% of the N<sub>2</sub>O was reduced to N<sub>2</sub> for more than 600 h in the presence of 500 ppm SO<sub>2</sub>. SO<sub>2</sub> was not oxidized to SO<sub>3</sub> over the catalyst and this caused the tolerance of this catalyst to the SO<sub>2</sub> presence, according to the above authors.

The N<sub>2</sub>O reduction by CO [6] or CH<sub>4</sub> [7] was examined in the absence of O<sub>2</sub>. NH<sub>3</sub> has also been used as a reducing agent [8,9] resulting in high N<sub>2</sub>O conversions over Ru and Rh zeolitic catalysts. However, the presence of 3% O<sub>2</sub> caused a significant inhibition of the reaction.

Catalytic decomposition has been studied more than the SCR of N<sub>2</sub>O over different catalytic systems [3,10–18]. Parameters that affect the decomposition rate over an active site are the type of the support and the presence of other gases (O<sub>2</sub>, H<sub>2</sub>O, SO<sub>2</sub>). Most of the catalysts under realistic reaction conditions exhibited low activity [1]. The presence of O<sub>2</sub> and other gases such as SO<sub>2</sub> and H<sub>2</sub>O that typically exist in flue gas streams inhibited the catalysts' activity [14,17,19,20]. Rh supported on TiO<sub>2</sub> and on ZSM-5 lost most of its activity when O<sub>2</sub>, H<sub>2</sub>O or SO<sub>2</sub> was added to the feed according to Centi *et al.* [14]. Lower N<sub>2</sub>O decomposition rates were measured

\* To whom correspondence should be addressed.  
e-mail: efthimia@alexandros.cperi.certh.gr

by Chang *et al.* [15] in the presence of excess oxygen over Ru/ZSM-5. The above authors postulated that at low temperatures  $O_2$  desorption is the rate-limiting step; therefore, high  $O_2$  concentrations suppress the extent of the reaction.

The effect of the type of the support and the Rh dispersion on the  $N_2O$  decomposition was studied by Yazaki *et al.* [21]. Rh supported on USZ and alumina was more active than that supported on FSM-16,  $CeO_2$ ,  $ZrO_2$  and  $La_2O_3$ . The mechanism of  $O_2$  desorption during the  $N_2O$  decomposition over Rh/USZ was the Langmuir–Hinshelwood, and reaction-assisted desorption of  $O_2$  occurred at low temperatures [22,23].

$N_2O$  decomposition is inhibited by  $SO_2$  because  $SO_2$  is oxidized to  $SO_3$  and it subsequently forms sulfates [14,17]. However, Perez-Ramirez *et al.* [24] reported that the presence of Mg in Ni-HTlc and Co-HTlc catalysts prevents the deactivation of the catalysts due to the preferential adsorption of  $SO_2/SO_3$  on the  $MgO$  phase. In this way, the active sites are free for the  $N_2O$  reduction. The  $N_2O$  decomposition rate is higher in a dry stream than that in a wet one [10–13,18,19]. The loss of activity due to the  $H_2O$  presence is reversible. This behavior was attributed to the competitive adsorption of  $H_2O$  and  $N_2O$  on the catalytic surface. On the other hand, Zeng and Pang [13] postulated that the deactivation of Ru/ $Al_2O_3$  by  $H_2O$  is the result of chemical constituent changes (acidity–basicity of the catalyst).

Previous experimental works have shown that the presence of oxygen that typically exists in flue gases derived from fluidized bed combustors inhibits the activity of most catalysts. The commercial application of  $N_2O$  reduction catalysts requires catalytic activities not only in the presence of oxygen, but also in the presence of other poison gases such as  $H_2O$  and  $SO_2$ . The purpose of this work is to present the performance of a series of metal-based catalysts efficient for the  $N_2O$  reduction. Catalysts based on different metal active sites and supported on different metal oxide carriers

were tested. We chose to add traces of propene and excess  $O_2$  in the feed of most experiments of this study because the former gas is typically employed in SCR studies and the latter one is present in most flue gases. Finally, the resistance of the most promising catalysts to the presence of poison gases ( $H_2O$ ,  $SO_2$ ) was examined.

## 2. Experimental

### 2.1. Materials

A series of Rh-, Ru-, Pd-, In-, Fe-, Cu-, and Co-based on alumina catalysts were prepared using the dry impregnation technique.  $\gamma$ -alumina was supplied by Engelhard in extrudates which were crushed and sieved to separate the particles of 180–355  $\mu m$ . In order to examine the effect of the type of the support on the catalyst performance we deposited Rh on various supports, namely  $SiO_2$  (Grace),  $TiO_2$  (Norton),  $ZrO_2$  (Norton) and hydrotalcite  $MgAl_2(OH)_8 \cdot H_2O$  (Condea). The  $MgO/Al_2O_3$  ratio was equal to 7/3 in the last sample. Before the impregnation, hydrotalcite was calcined at 650 °C for 2 h in order to remove the water content. All supports were in the same particle size with  $\gamma$ -alumina. Water solutions of the corresponding metal salts were impregnated on the carriers. Following the impregnation, the catalysts were dried at 120 °C for 2 h and then they were calcined at 600 °C or 500 °C, under air flow. The metal content in each of the catalysts was measured by the ICP/AES technique. A list of catalysts is given in table 1 along with the calcination conditions, the percentage of the active sites and the precursor salt.

### 2.2. Experimental setup

Reactivity experiments were carried out in a laboratory-scale reaction unit. The unit consists of the feed gas

Table 1  
List of prepared catalysts

Catalyst	Calcination conditions	Metal loading	Metal salt
Rh/ $Al_2O_3$	600 °C/9 h with air	2% Rh	$RhCl_3$
Rh/ $ZrO_2$	600 °C/9 h with air	2% Rh	$RhCl_3$
Rh/ $TiO_2$	600 °C/9 h with air	2% Rh	$RhCl_3$
Rh/ $SiO_2$	600 °C/9 h with air	2% Rh	$RhCl_3$
Rh/HTlc7	600 °C/9 h with air	1.6% Rh	$RhCl_3$
Ru/ $Al_2O_3$	550 °C/6 h with air	2% Ru	$RuCl_3$
Pd/ $Al_2O_3$	500 °C/6 h with air	2% Pd	$PdCl_3$
Fe/ $Al_2O_3$	500 °C/6 h with air	2% Fe	$Fe(NO_3)_3$
Co/ $Al_2O_3$	500 °C/6 h with air	1% Co	$Co(NO_3)_2$
In/ $Al_2O_3$	600 °C/6 h with air	2% In	$In(NO_3)_3$
Cu/ $Al_2O_3$	500 °C/6 h with air	2% Cu	$Cu(NO_3)_2$

system, a fixed-bed reactor and the gas analysis system. Gases of standard composition were initially mixed and then introduced into a quartz reactor of 1.7 cm i.d. The composition of the reactive gas during the  $N_2O$  reduction experiments was 500 ppm  $N_2O$ , 1000 ppm hydrocarbon, 5%  $O_2$ , 0 or 50 ppm  $SO_2$ , 0 or 10%  $H_2O$  in He. Propene, propane or methane was used as reductant. When water was added to the reactive gas mixture, pure He was saturated with water at 50°C and the  $H_2O/He$  gas mixture was mixed with the other gases. In this case, all lines prior to the reactor were heated at 100°C to avoid any water condensation. The reactor loading was 1 g and the flow rate was 500 cc/mm. As a result, the catalyst to flow ratio (W/F) was 0.12 g  $cm^{-3}$ . More details about the reaction unit can be found elsewhere [25].

The composition of the exit gas stream was analyzed by a series of analyzers and a gas chromatograph (GC). The concentration of the following gases was measured by the analyzers:  $N_2O$  (NDIR, VIA-510 Horiba),  $NO_x$  (Chemiluminescence, Thermo Environmental 42C-HL),  $CO_2$  (NDIR, VIA-510 Horiba), CO (NDIR, VIA-510 Horiba),  $O_2$  (paramagnetic, MPA-510 Horiba) and  $SO_2$  (NDUV, AR 3000 Anarad). Gas samples were automatically injected in a HP GC equipped with TCD and FID detectors. The former detector was used for the  $N_2$  and the latter one for hydrocarbon concentration measurements.

### 3. Results and discussion

#### 3.1. Effect of active site on the $N_2O$ reduction (presence of $C_3H_6$ and $O_2$ )

Pure  $\gamma$ -alumina and alumina-based catalysts were initially tested as catalysts for the  $N_2O$  reduction in the presence of  $C_3H_6$  and  $O_2$ . The experimental data of figure 1 show that unpromoted alumina exhibits very low activity for the reduction of  $N_2O$  to  $N_2$ . The deposition of an active metal on alumina enhanced the activity. Complete conversion of  $N_2O$  to  $N_2$  was observed over  $Rh/Al_2O_3$  and  $Ru/Al_2O_3$  at 480°C. The other alumina-based catalysts exhibited significantly lower activity at temperatures lower than 600°C. Among these catalysts  $Fe/Al_2O_3$  was the most active and  $Co/Al_2O_3$  the least active. The activity of the catalysts shown in figure 1 follows the order  $Rh \geq Ru > Fe > Pd > In > Co$ . The shape of the  $N_2O$  conversion versus temperature curves (solid lines) is different from the typical  $NO_x$  conversion versus temperature curve [26–28]. At low temperatures both curves follow a sigmoidal pattern; however, at higher temperatures the  $N_2O$  conversion reaches 100% and remains stable, while the  $NO_x$  conversion drops. On the other hand, the shape of the propene conversion versus temperature curves (dashed lines) is sigmoidal both in the  $NO_x$  and  $N_2O$  reduction experiments. Propene is consumed very fast over  $Pd/Al_2O_3$ , a

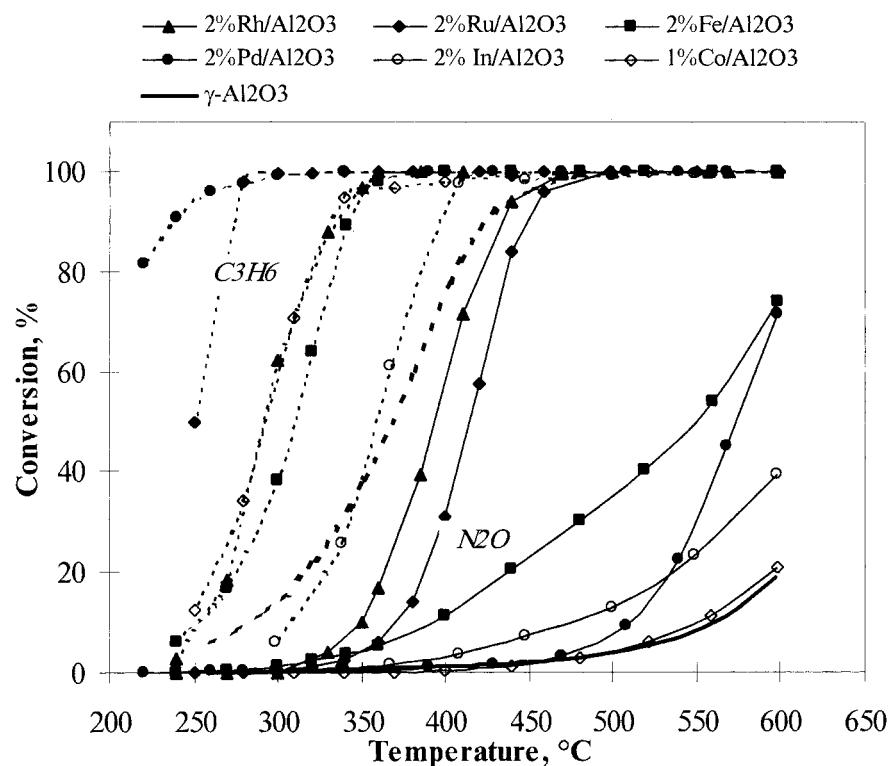


Figure 1. Conversion of  $N_2O$  (solid lines) and  $C_3H_6$  (dashed lines) over alumina and alumina-based catalysts. Feed: 500 ppm  $N_2O$ , 1000 ppm  $C_3H_6$ , 5%  $O_2$ , balance He.

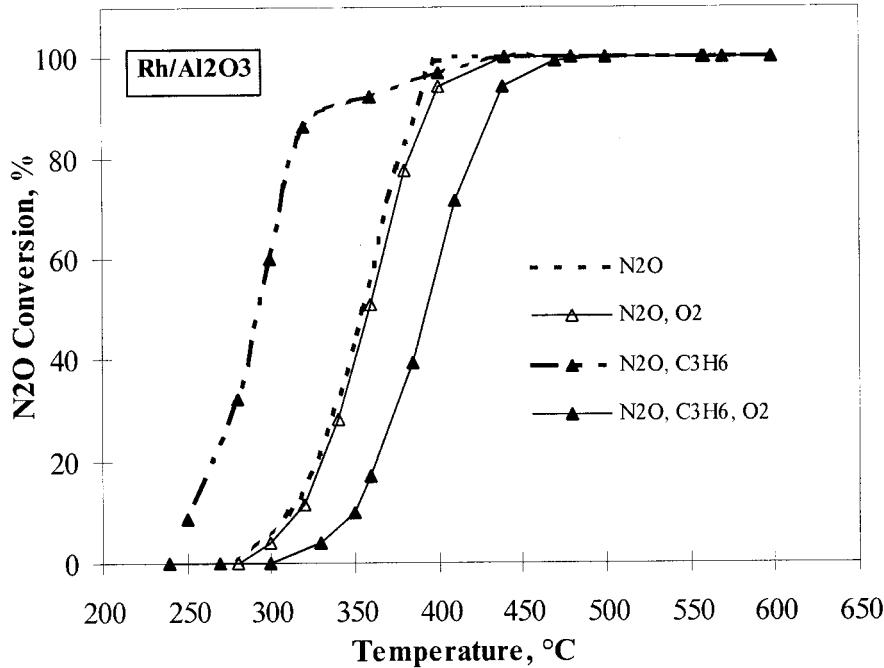


Figure 2. Conversion of  $N_2O$  to  $N_2$  over  $Rh/Al_2O_3$  catalyst, in the presence and in the absence of  $O_2$  and  $C_3H_6$ . Feed: 500 ppm  $N_2O$ , 0 or 1000 ppm  $C_3H_6$ , 0 or 5%  $O_2$ , balance He.

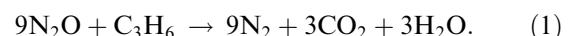
well-known oxidizing catalyst, followed by  $Ru/Al_2O_3$ . The propene conversion curves over  $Rh/Al_2O_3$ ,  $Co/Al_2O_3$  and  $Fe/Al_2O_3$  almost coincide, while propene is burned over  $In/Al_2O_3$  and pure  $Al_2O_3$  at higher temperatures. However, over all samples of figure 1 propene reaches complete conversion at temperatures significantly lower than those of complete  $N_2O$  reduction. As a result, at temperatures higher than that of complete propene consumption, the reductant is present only in a part of the catalytic bed. When the temperature of reaction rises the portion of the catalytic bed that sees propene decreases. Given that under these conditions complete reduction of  $N_2O$  is observed, we postulate that in the main  $N_2O$  is catalytically decomposed to  $N_2$ .

### 3.2. Role of $O_2$ and reductant on the $N_2O$ reduction

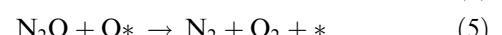
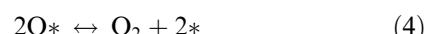
We performed a series of experiments aiming at the elucidation of the  $O_2$  and  $C_3H_6$  role during the  $N_2O$  reduction. We chose the two most active catalysts of figure 1, namely  $Rh/Al_2O_3$  and  $Ru/Al_2O_3$ , for these experiments and we varied the feed composition. The dashed line in figure 2 shows the conversion of  $N_2O$  to  $N_2$  in the absence of both  $O_2$  and  $C_3H_6$  over  $Rh/Al_2O_3$ . The light-off temperature is 300 °C and at 400 °C more than 90% of  $N_2O$  is reduced. Other researchers, as well, observed similar experimental data for the catalytic decomposition of  $N_2O$  to  $N_2$ . Specifically, Yuzaki *et al.* [29] and Schulz *et al.* [17] measured complete decomposition of  $N_2O$  to  $N_2$  at 400 °C over  $Rh/Al_2O_3$ . The same conversion of  $N_2O$  to  $N_2$  was also measured over zeolites and hydrotalcites [10,30].

Addition of  $O_2$  in the feed (figure 2) had no influence on the decomposition of  $N_2O$  to  $N_2$ . This implies that oxygen is not adsorbed on the catalyst competitively with  $N_2O$ . Moreover, the presence of 5%  $O_2$  does not inhibit the desorption of  $O_2$  derived from the  $N_2O$  reduction. Satsuma *et al.* [7] studied the  $N_2O$  decomposition over various metal oxide catalysts in the presence and in the absence of  $O_2$ . They classified the metal oxides according to the  $O_2$  effect on the  $N_2O$  reduction into two categories: those that were not affected and those that were inhibited by the oxygen presence in the feed. Alumina was among the materials of the former category.

We replaced  $O_2$  with  $C_3H_6$  in the feed (absence of  $O_2$ ) and we observed a significant enhancement of the  $N_2O$  conversion to  $N_2$  expressed as a shift of the  $N_2O$  conversion *versus* temperature curve to lower temperatures. The catalytic reduction of  $N_2O$  by propene proceeds via the reaction



The catalytic decomposition of  $N_2O$  follows the decomposition mechanism (1) described by the reactions



where  $*$  is an active site.

In the absence of  $O_2$  in the bulk phase, propene is used to remove the surface oxygen formed from the  $N_2O$

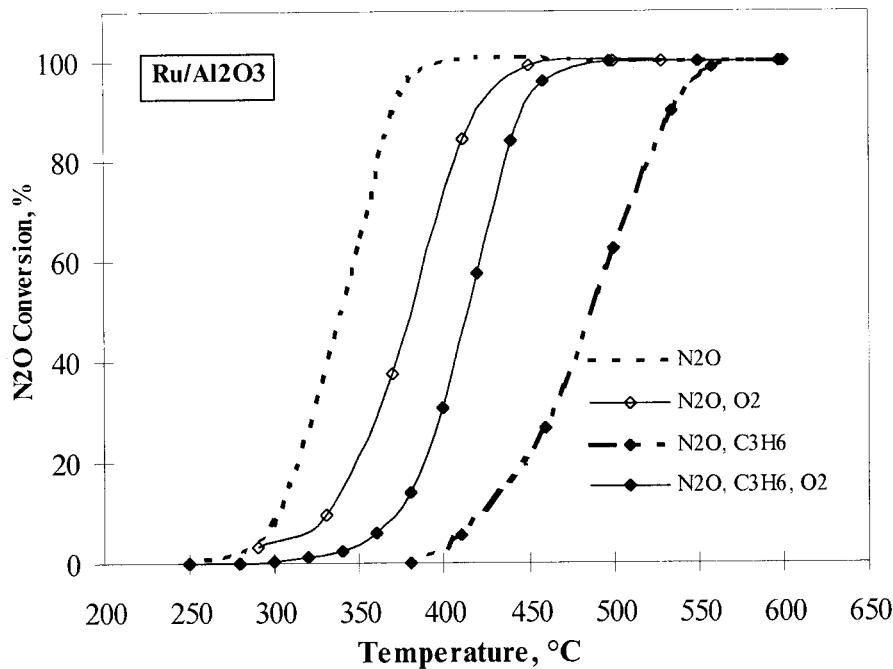
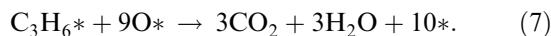
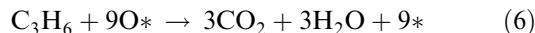


Figure 3. Conversion of  $N_2O$  to  $N_2$  over  $Ru/Al_2O_3$  catalyst, in the presence and in the absence of  $O_2$  and  $C_3H_6$ . Feed: 500 ppm  $N_2O$ , 0 or 1000 ppm  $C_3H_6$ , 0 or 5%  $O_2$ , balance He.

decomposition according to the reactions



The “cleanup” of the catalytic surface by propene (in the bulk phase or adsorbed) favors the dissociative adsorption of  $N_2O$ . Moreover, propene can modify the oxidation stage of the Rh active sites leading to partially reduced sites. During the selective catalytic reduction of  $NO_x$  with propene over  $Rh/Al_2O_3$ , partial reduction of  $Rh_2O_3$  was observed in our previous work [31]. This was verified by XPS measurements performed in this work, where we observed partial reduction of Rh as a result of the  $N_2O$  presence. This reduction was more pronounced in the absence of  $O_2$ . Therefore, the presence of propene in the feed may benefit the  $N_2O$  reduction to  $N_2$ , both consuming oxygen derived from  $N_2O$  and reducing the active sites.

When oxygen was added to the feed (feed:  $N_2O$ ,  $C_3H_6$  and  $O_2$ ), the  $N_2O$  versus temperature curve was shifted toward higher temperatures by about 80 °C as compared with experiments where  $N_2O/He$  or  $N_2O/C_3H_6/He$  were fed (figure 2). When both bulk  $O_2$  and  $N_2O$  coexist in the feed, propene adsorbed on the active sites is selectively oxidized by  $O_2$ , thus inhibiting the  $N_2O$  reduction. In the absence of  $O_2$ ,  $N_2O$  is catalytically decomposed to  $N_2$  and catalytically reduced by  $C_3H_6$ . However, in the presence of  $O_2$  the latter mechanism of  $N_2$  formation is inhibited and  $N_2O$  competes with  $C_3H_6$  for the same sites.

In figure 3 we present experimental results for different feeds over  $Ru/Al_2O_3$ . The  $N_2O$  conversion curves

over  $Ru/Al_2O_3$  and  $Rh/Al_2O_3$  were similar when the feed contained  $N_2O$  only. However, addition of  $O_2$  in the feed caused a shift of the  $N_2O$  decomposition curve to higher temperatures (*ca.* 60 °C) over the former sample and had no effect over the latter one. Given that both fresh samples are fully oxidized, the presence of  $O_2$  in the feed is not expected to modify their oxidation state. As a result, we attribute the difference in the  $N_2O$  conversion curves between the two alumina-based samples to the adsorption characteristics on the metal active sites. We believe that  $O_2$  is adsorbed on Ru more strongly than on Rh, thus inhibiting the  $N_2O$  reduction in the former sample. In accordance to these results, Zeng *et al.* [13] noticed that the inhibition caused by  $O_2$  depended on the temperature.

Another interesting difference between the performance of  $Ru/Al_2O_3$  and  $Rh/Al_2O_3$  is the significant inhibition of the  $N_2O$  reduction by  $C_3H_6$  over the former sample (figure 3), while the inverse was observed over the latter one (figure 2). Specifically, complete conversion of  $N_2O$  was measured above 560 °C in the presence of  $N_2O$  and  $C_3H_6$ , while in the absence of  $C_3H_6$  this temperature was 400 °C over  $Ru/Al_2O_3$ . XRD and XPS measurements of this work agree with previous measurements [13] that fresh Ru supported on alumina is in the form of  $RuO_2$  (oxidation state +4). Furthermore, our XPS measurements showed that when  $N_2O$  and  $C_3H_6$  exist in the feed, Ru is reduced to its metallic form, while addition of  $O_2$  inhibits the reduction of ruthenium oxides. Chang and coworkers [15,16] support that  $RuO_2$  and its related oxides  $RuO_x$  are good electron conductors with high chemical stability.

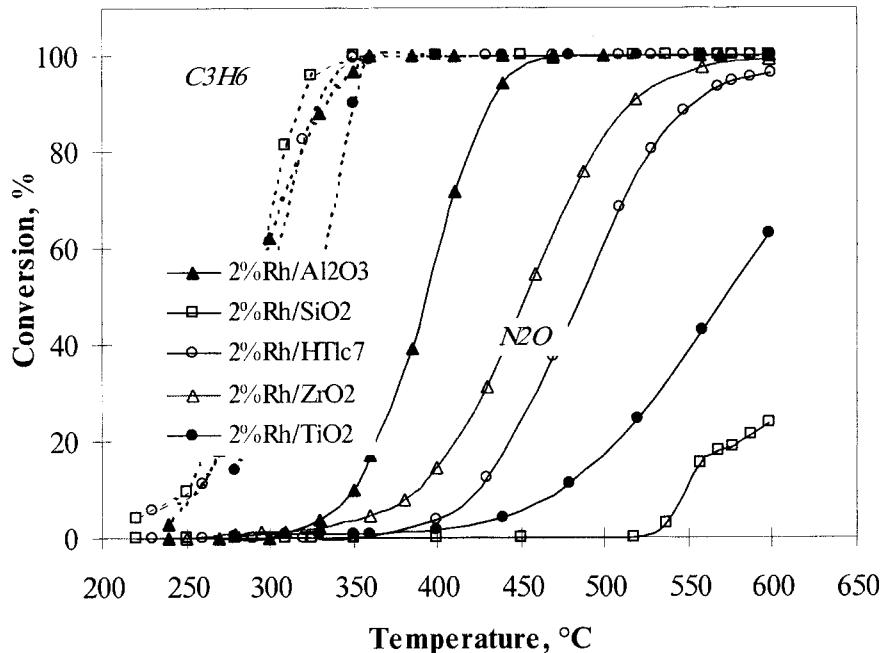


Figure 4. Conversion of  $N_2O$  (solid lines) and  $C_3H_6$  (dashed lines) over Rh catalysts impregnated on different supports. Feed: 500 ppm  $N_2O$ , 1000 ppm  $C_3H_6$ , 5%  $O_2$ , balance He.

As a result, these oxides are the active components for the  $N_2O$  decomposition because  $Ru^{+3}/Ru^{+4}$  are effective for the N–C weakening and charge transfer during the  $N_2O$  decomposition. Therefore, we believe that  $C_3H_6$  in the absence of  $O_2$  reduces the  $Ru^{+3}/Ru^{+4}$  sites. These reduced sites of Ru are inactive for the  $N_2O$  decomposition.

The inhibition of the  $N_2O$  reduction over  $Ru/Al_2O_3$ , caused by the addition of propene in the feed, moderated upon the addition of 5%  $O_2$  (figure 3). We attribute this behavior to the oxidation of propene by bulk  $O_2$ . In this way the oxidation state of the active sites remains almost unaffected by the propene presence, but competitive adsorption between  $N_2O$ ,  $C_3H_6$  and  $O_2$  leads to lower  $N_2O$  conversions than in the experiments where  $N_2O$  or  $N_2O$  and  $O_2$  existed in the feed.

### 3.3. Effect of support on Rh-based catalysts

The effect of the carrier on the performance of Rh-based catalysts was studied, impregnating Rh on the following supports:  $Al_2O_3$ ,  $SiO_2$ ,  $TiO_2$ ,  $ZrO_2$  and calcined hydrocalcite (HTlc7). We chose Rh as the active site since this metal was the most active between the alumina-based catalysts examined in figure 1. In figure 4 we present the variation of the  $N_2O$  conversion versus temperature curve with the type of the support. The feed in these experiments consisted of 500 ppm  $N_2O$ , 1000 ppm  $C_3H_6$  and 5%  $O_2$  in He.  $Rh/Al_2O_3$  exhibited the highest activity among the catalysts of this figure. Complete conversion of  $N_2O$  to  $N_2$  was measured over this sample at 450 °C. The corresponding

temperature over  $Rh/ZrO_2$  was 550 °C and that over  $Rh/HTlc7$  was 600 °C. The activities of other catalysts  $Rh/TiO_2$  and  $Rh/SiO_2$  were lower. In accordance with the results of figure 1, the reductant was consumed at low temperatures where the  $N_2O$  reduction was negligible.

Centi *et al.* [14] studied the effect of the type of the support on noble-metal based catalysts for the decomposition of  $N_2O$ . They compared ZSM-5 with metal oxide carriers and they postulated that ZSM-5 performs as the best carrier, followed by  $TiO_2$ ,  $Al_2O_3$  and  $ZrO_2$ . They attributed differences in the activity to the variation of the Rh dispersion on different supports. Experimental results of Yuzaki *et al.* [29] agree with the results of our study.

$Rh/USY$  and  $Rh/Al_2O_3$  exhibited the highest activity for the  $N_2O$  decomposition. The activity of the supports varied in the following order:  $USY > Al_2O_3 > ZrO_2 > CeO_2 > FSM - 16 \gg La_2O_3$ .

### 3.4. Effect of the reducing agent

In most of the previous experiments propene was present in the feed. However, the presence of 1000 ppm  $C_3H_6$  in the feed decreased the  $N_2O$  conversion when 5%  $O_2$  coexisted in the feed (figure 2). A general remark from the previous experimental data of this work is that propene was consumed at low temperatures where the conversion of  $N_2O$  is negligible. Given that propene, an unsaturated hydrocarbon, is easily burned, we chose to examine the effect of two saturated hydrocarbons ( $CH_4$  and  $C_3H_8$ ) on the  $N_2O$  reduction. These experiments were carried out over the most active

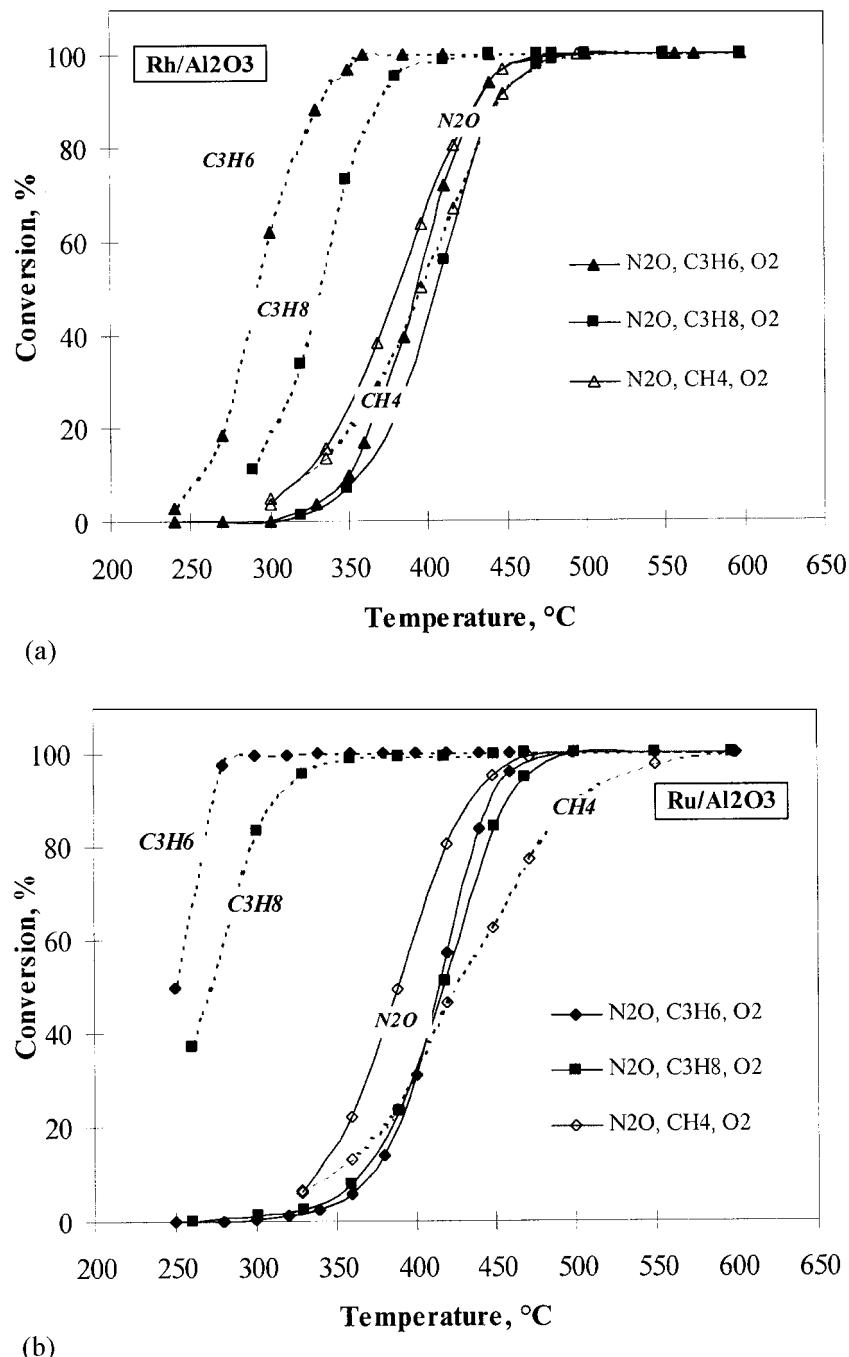


Figure 5. Effect of the type of the reducing agent on the  $N_2O$  conversion to  $N_2$ , over Rh/Al<sub>2</sub>O<sub>3</sub> (a) and Ru/Al<sub>2</sub>O<sub>3</sub> (b). Feed: 500 ppm  $N_2O$ , 1000 ppm  $C_3H_6$  or  $C_3H_8$  or  $CH_4$ , 5%  $O_2$ , balance He.

catalysts, namely Rh/Al<sub>2</sub>O<sub>3</sub> and Ru/Al<sub>2</sub>O<sub>3</sub>, using 1000 ppm of each hydrocarbon, 500 ppm  $N_2O$  and 5%  $O_2$ .

In figure 5 we present experimental results when methane, propane and propene are present in the feed over Rh/Al<sub>2</sub>O<sub>3</sub> and Ru/Al<sub>2</sub>O<sub>3</sub>. A small shift of the  $N_2O$  curve to higher temperatures was observed over both catalysts when propane replaced propene in the feed. On the other hand, propane was oxidized at higher temperatures than propene was. The inverse behavior was observed when methane was fed in the

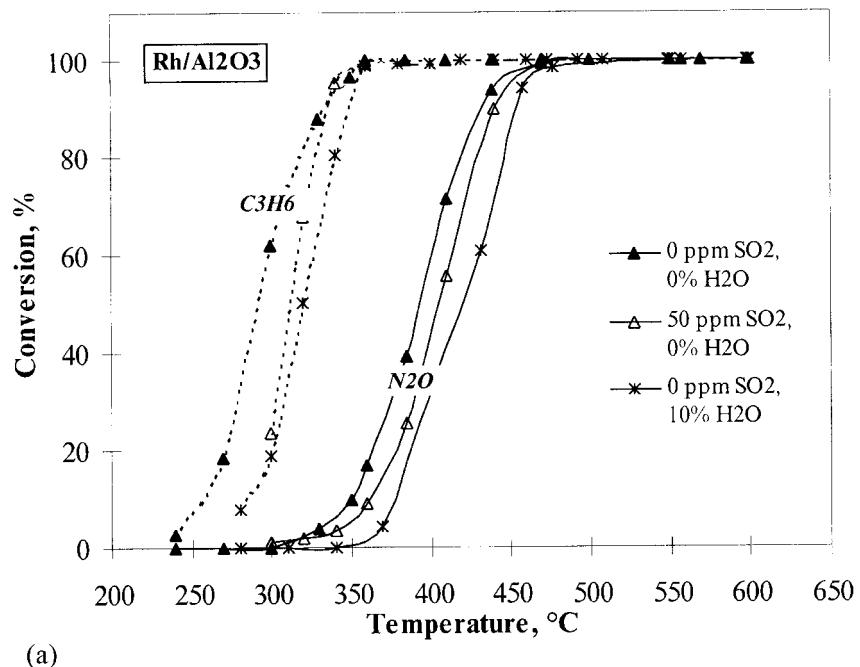
reactor. The light-off temperature was shifted to lower values as compared with the experiments where the other two reductants were used over both catalysts. At a given temperature the  $N_2O$  conversion was equal to or higher than that of  $CH_4$ . This implies that methane is adsorbed and burned at higher temperatures than the other two reductants. Anyway, the type of the hydrocarbon did not affect the  $N_2O$  reduction curves significantly. These results confirm our argument in section 3.1 that  $N_2O$  reduction takes place mainly

according to a decomposition reaction mechanism even in the presence of a hydrocarbon. Finally, the temperature of the hydrocarbon activation over Rh/ $Al_2O_3$  and Ru/ $Al_2O_3$  followed the order:  $C_3H_6 < C_3H_8 < CH_4$ .

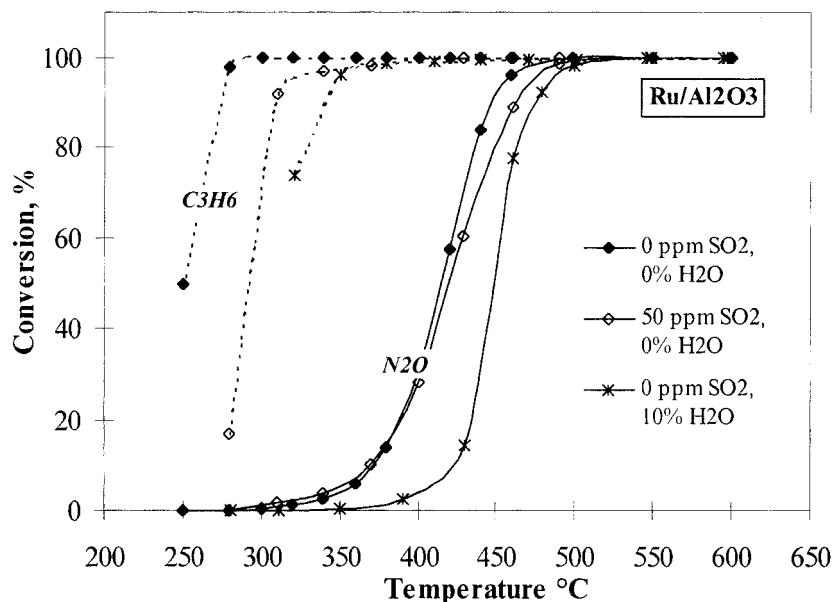
### 3.5. $SO_2$ and $H_2O$ effect on the $N_2O$ reduction

The performance of the most promising catalysts of this study (Rh/ $Al_2O_3$  and Ru/ $Al_2O_3$ ) under realistic reaction conditions was examined by adding  $SO_2$  and

$H_2O$  in feed that consisted of 500 ppm  $N_2O$ , 1000 ppm  $C_3H_6$ , 5%  $O_2$  in He. We tested the influence of the  $H_2O$  and  $SO_2$  presence initially separately, and then simultaneously. Experimental results for Rh/ $Al_2O_3$  and Ru/ $Al_2O_3$  are presented in figures 6(a) and 6(b), respectively. The presence of 50 ppm  $SO_2$  in the feed caused a small shift of the  $N_2O$  curve to higher temperatures over Rh/ $Al_2O_3$ , while the same was observed over Ru/ $Al_2O_3$  at high temperatures. The temperature where complete conversion of  $N_2O$  was measured did not



(a)



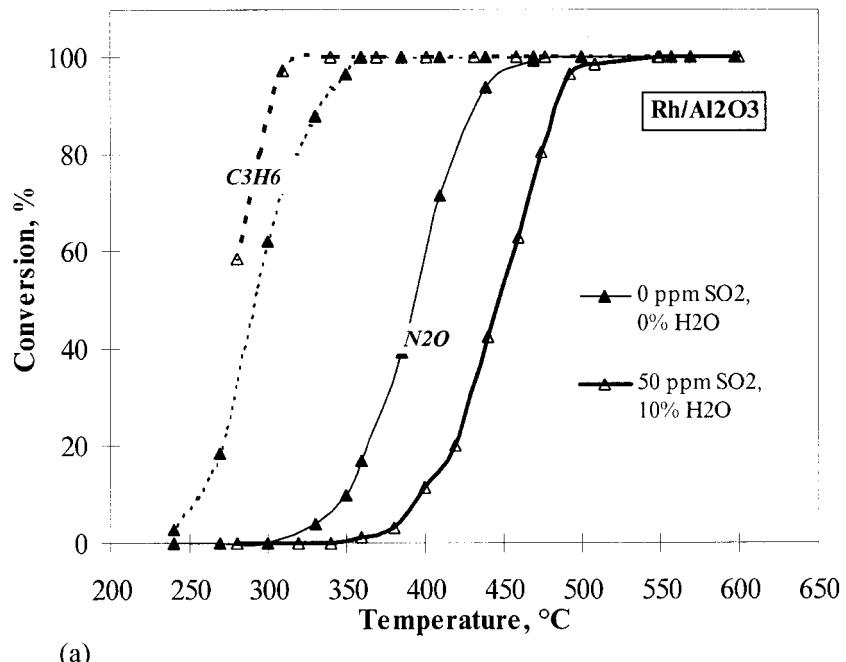
(b)

Figure 6. Effect of the presence of  $SO_2$  and  $H_2O$  on the  $N_2O$  conversion to  $N_2$ , over Rh/ $Al_2O_3$  (a) and Ru/ $Al_2O_3$  (b). Feed: 500 ppm  $N_2O$ , 1000 ppm  $C_3H_6$ , 0 or 50 ppm  $SO_2$ , 0 or 10%  $H_2O$ , 5%  $O_2$ , balance He.

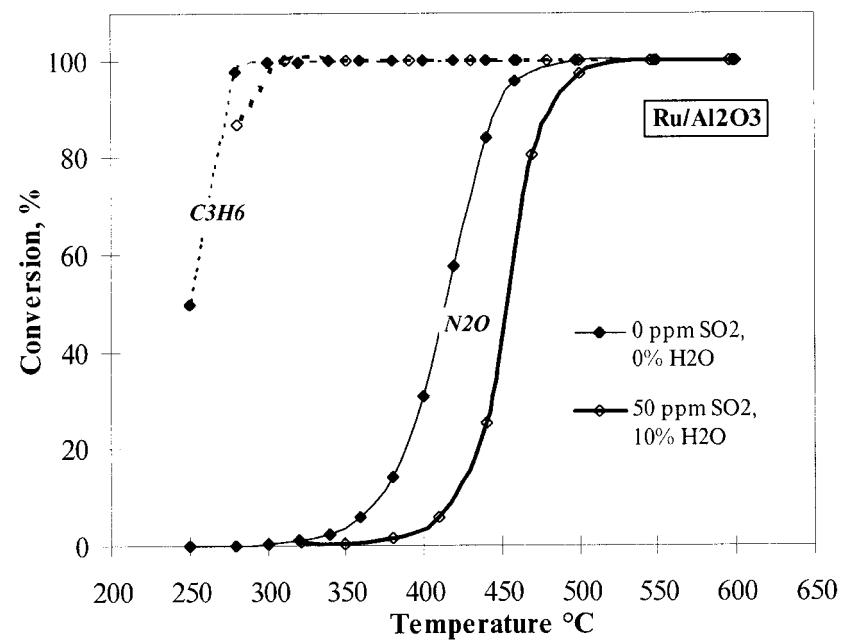
change significantly after the addition of  $SO_2$  over both catalysts. These data are in agreement with experiments where  $N_2O$  was catalytically decomposed in the presence of  $SO_2$  [14,17]. Noble metals enhance the  $SO_2$  oxidation to  $SO_3$ , resulting in the formation of sulfates species. These species are stable on the catalytic surface up to 480–500 °C. Further increase of the reaction temperature favors their decomposition and, thus, the clean up of the catalytic surface. As a result at temperatures higher than

about 480 °C the experimental data in the presence and in the absence of  $SO_2$  are similar.

The presence of 10%  $H_2O$  in the feed inhibited the conversion of  $N_2O$  to  $N_2$  more than  $SO_2$  did. This inhibition was more pronounced at lower temperatures. The same trend was observed for the  $C_3H_6$  conversion *versus* temperature curves. Similar behavior was noticed by other researchers during the catalytic decomposition of  $N_2O$  over  $Ru/Al_2O_3$ , in the presence of  $H_2O$  [13,19].



(a)



(b)

Figure 7. Effect of the simultaneous presence of  $SO_2$  and  $H_2O$  on the  $N_2O$  conversion to  $N_2$ , over  $Rh/Al_2O_3$  (a) and  $Ru/Al_2O_3$  (b). Feed: 500 ppm  $N_2O$ , 1000 ppm  $C_3H_6$ , 0 or 50 ppm  $SO_2$ , 0 or 10%  $H_2O$ , 5%  $O_2$ , balance He.

Wang *et al.* [13] attributed this phenomenon to the competitive adsorption of N<sub>2</sub>O and H<sub>2</sub>O on the same active sites since both molecules are polar. At lower temperatures the coverage of active sites by adsorbed water reduced the number of these sites that are available for the N<sub>2</sub>O reduction. At higher reaction temperatures the H<sub>2</sub>O desorption was favored and the rate of the N<sub>2</sub>O decomposition increased, reaching that of the H<sub>2</sub>O-free experiments. Another explanation for the inhibition caused by H<sub>2</sub>O was given by Zeng *et al.* [13]. They postulated that RuO<sub>2</sub> formed new phases, such as oxyhydroxides. These hydroxyl groups were retained on the surface and changed the acidity–basicity of the catalytic surface leading to the change of the electronic structure of the active RuO<sub>2</sub> phase and, as a result, decreased the catalytic activity.

In figures 7(a) and 7(b) we compare the conversion *versus* temperature curves for two feeds, one SO<sub>2</sub>-free and H<sub>2</sub>O-free and one containing both gases over Rh/Al<sub>2</sub>O<sub>3</sub> and Ru/Al<sub>2</sub>O<sub>3</sub>, respectively. The coexistence of SO<sub>2</sub> and H<sub>2</sub>O caused a shift of the N<sub>2</sub>O conversion curves to higher temperatures of about 60 and 40 °C over Rh/Al<sub>2</sub>O<sub>3</sub> and Ru/Al<sub>2</sub>O<sub>3</sub>, respectively. Complete conversion to N<sub>2</sub> was noticed above 500 °C, over both catalysts. A similar inhibition effect on the reduction of N<sub>2</sub>O caused by coexistence of SO<sub>2</sub> and H<sub>2</sub>O in the feed was observed by Centi *et al.* [3] over Fe/ZSM-5 at low temperatures, while at temperatures higher than 400 °C the catalyst maintained its initial activity. The above authors attributed this behavior to the inability of the catalyst to oxidize SO<sub>2</sub> to SO<sub>3</sub> after the initial deactivation step.

#### 4. Conclusions

Rh and Ru supported on  $\gamma$ -alumina were the most promising catalysts of this study for the N<sub>2</sub>O reduction in the presence of C<sub>3</sub>H<sub>6</sub> traces and excess O<sub>2</sub>. Complete reduction of N<sub>2</sub>O to N<sub>2</sub> was measured at temperatures that varied with the composition of the feed. In the absence of O<sub>2</sub>, C<sub>3</sub>H<sub>6</sub> enhanced the N<sub>2</sub>O reduction over Rh/Al<sub>2</sub>O<sub>3</sub>, but inhibited that over Ru/Al<sub>2</sub>O<sub>3</sub>. This was attributed to differences in the activity of fully oxidized and partially reduced metal sites. Partially reduced Rh and fully oxidized Ru are efficient catalysts for the N<sub>2</sub>O reduction. Differences on the N<sub>2</sub>O conversion *versus* time curves between the above two samples after the addition of O<sub>2</sub> was attributed to the adsorption coefficients of O<sub>2</sub>.

Comparison of the N<sub>2</sub>O conversion *versus* temperature curves using hydrocarbon-containing feeds showed that the type of the hydrocarbon (CH<sub>4</sub>, C<sub>3</sub>H<sub>8</sub> or C<sub>3</sub>H<sub>6</sub>) did not significantly affect the experimental results. Moreover, C<sub>3</sub>H<sub>8</sub> or C<sub>3</sub>H<sub>6</sub> was completely consumed at low temperatures where N<sub>2</sub>O conversion was negligible. These results imply that N<sub>2</sub>O is decomposed to N<sub>2</sub> rather

than reduced by the hydrocarbon when O<sub>2</sub> is in excess in the feed.

The addition of SO<sub>2</sub> and/or H<sub>2</sub>O in the feed shifted the N<sub>2</sub>O *versus* temperature curve to higher temperatures. We attributed this behavior to the formation of sulfates that decompose at *ca.* 500 °C and to the competitive adsorption of N<sub>2</sub>O and H<sub>2</sub>O on the same sites.

#### Acknowledgment

The authors wish to thank Professor J.L. Figueiredo for the XPS measurements in the Laboratory of Catalysis and Materials in the Faculty of Engineering of the University of Porto, Portugal. The Commission of the European Community funded this work, under Contract ENK5-CT-1999-00001.

#### References

- [1] F. Kapteijn, J. Rodriguez-Mirasol and J.A. Moulijn, *Appl. Catal. B* 9 (1996) 25.
- [2] K. Yamada, C. Pophal and K. Segawa, *Micropor. Mesopor. Mater.* 21 (1998) 549.
- [3] G. Centi and F. Vazzana, *Catal. Today* 53 (1999) 683.
- [4] K. Yamada, S. Kondo and K. Segawa, *Micropor. Mesopor. Mater.* 35-36 (2000) 227.
- [5] C. Pophal, T. Yogo, K. Yamada and K. Segawa, *Appl. Catal.* 16 (1998) 177.
- [6] J.H. Holles, M.A. Switzer and R.J. Davis, *J. Catal.* 190 (2000) 247.
- [7] A. Satsuma, H. Maeshima, K. Watanabe, K. Suzuki and T. Hattori, *Catal. Today* 63 (2000) 347.
- [8] K. Aika and K. Oshihara, *Catal. Today* 29 (1996) 123.
- [9] M. Mauvezin, G. Delahay, B. Coq and S. Kieger, *Appl. Catal. B* 23 (1999) L79.
- [10] J. Oi, A. Obuchi, A. Ogata, G.R. Bamwenda, R. Tanaka, T. Hibino and S. Kushiyama, *Appl. Catal. B* 13 (1997) 197.
- [11] S. Kannan, *Appl. Clay Sci.* 13 (1998) 347.
- [12] J.N. Armor, T.A. Braymer, T.S. Farris, Y. Li, F.P. Petrocelli, E.L. Weist, S. Kannan and C.S. Swamy, *Appl. Catal. B* 7 (1996) 397.
- [13] H.C. Zeng and X.Y. Pang, *Appl. Catal. B* 13 (1997) 113.
- [14] G. Centi, A. Galli, B. Montanari, S. Perathoner and A. Vaccari, *Catal. Today* 35 (1997) 113.
- [15] Y.-F. Chang, J.G. McCarty, E.D. Wachsman and V.L. Wong, *Appl. Catal. B* 4 (1994) 283.
- [16] Y.-F. Chang, J.G. McCarty and E.D. Wachsman, *Appl. Catal. B* 6 (1995) 21.
- [17] T.W. Dann, K.H. Schulz, M. Mann and M. Collings, *Appl. Catal. B* 6 (1995) 1.
- [18] J. Oi, A. Obuchi, G.R. Bamwenda, A. Ogata, H. Yagita, S. Kushiyama and K. Mizuno, *Appl. Catal. B* 12 (1997) 277.
- [19] X.F. Wang and H.C. Zeng, *Appl. Catal. B* 17 (1998) 89.
- [20] R.S. da Cruz, A.J.S. Mascarenhas and H.M.C. Andrade, *Appl. Catal. B* 18 (1998) 223.
- [21] K. Yuzaki, T. Yarimizu, K. Aoyagi, S. Ito and K. Kunimori, *Catal. Today* 45 (1998) 129.
- [22] S. Tanaka, K. Yuzaki, S. Ito, H. Uetsuka, S. Kameoka and K. Kunimori, *Catal. Today* 63 (2000) 413.
- [23] S. Tanaka, K. Yuzaki, S. Ito, S. Kameoka and K. Kunimori, *J. Catal.* 200 (2001) 203.
- [24] J. Pereuz-Ramirez, J. Overeijnden, F. Kapteijn and J.A. Moulijn, *Appl. Catal. B* 23 (1999) 59.

- [25] G.D. Lionta, S.C. Christoforou, E.A. Efthimiadis and I.A. Vasalos, Ind. Eng. Chem. Res. 35 (1996) 2508.
- [26] E.A. Efthimiadis, G.D. Lionta, S.C. Christoforou and I.A. Vasalos, Catal. Today 40 (1998) 15.
- [27] R. Burch and S. Scire, Appl. Catal. B 3 (1994) 295.
- [28] M.D. Amiridis, T. Zhang and R.J. Farrauto, Appl. Catal. B 10 (1996) 203.
- [29] K. Yuzaki, T. Yarimizu, K. Aoyagi, S. Ito and K. Kunimori, Catal. Today 45 (1998) 129.
- [30] Y. Li and J.N. Armor, Appl. Catal. B 3 (1993) 55.
- [31] E.A. Efthimiadis, S.C. Christoforou, A.A. Nikolopoulos and I.A. Vasalos, Appl. Catal. B 22 (1999) 91.